water

MDPI

Article

Growth, Oxidative Stress and Ability to Degrade Tetrabromobisphenol A of *Phanerochaete chrysosporium* in the Presence of Different Nano Iron Oxides

Ningjie Li [1,2,*], Jieyu Yu [1,2], Xiaojie Wang [1,2], Liu Chen [1,2], Hong Jiang [1,2] and Wenjie Zhang [1,2]

[1] Guangxi Key Laboratory of Environmental Pollution Control Theory and Technology, Guilin University of Technology, Guilin 541004, China
[2] Collaborative Innovation Center for Water Pollution Control and Water Safety in Karst Area, Guilin University of Technology, Guilin 541004, China
* Correspondence: echoningjie_333@126.com; Tel.: +86-07-73-589-6079

Abstract: In order to improve the performance of white rot fungi, especially the model species *Phanerochaete chrysosporium* in tetrabromobisphenol A (TBBPA) degradation, the strategy of synergizing *Phanerochaete chrysosporium* with nano iron oxides was considered; however, the effects of different nano iron oxides on *Phanerochaete chrysosporium* are still unknown. In this study, 20 nm γ-Fe_2O_3, 30 nm α-Fe_2O_3, 20 nm Fe_3O_4, and 200 nm Fe_3O_4 were used, and the fungal growth, oxidative stress, and ability to degrade TBBPA were monitored. The results showed that the addition of four nano iron oxides did not inhibit the growth of *Phanerochaete chrysosporium*. The effective antioxidant defense system of *Phanerochaete chrysosporium* could cope with almost all oxidative pressure induced by 200 nm Fe_3O_4. But when the size of nano iron oxide became significantly smaller or when the type of iron oxide changed from Fe_3O_4 to Fe_2O_3, a higher intracellular hydrogen peroxide (H_2O_2) content, lower intracellular superoxide dismutase (SOD) and catalase (CAT) activities and higher extracellular lactate dehydrogenase (LDH) activity were induced. When nano iron oxides synergized with *Phanerochaete chrysosporium*, the removal of TBBPA in all groups was slightly improved and mostly due to the degradation of TBBPA, with smaller iron oxides showing more enhancement for the degradation of TBBPA, while 200 nm Fe_3O_4 only enhanced the adsorption of TBBPA. The enhanced degradation of TBBPA showed no significant correlation with lignin-degrading enzyme activities but was closely correlated with the intracellular H_2O_2 concentration.

Keywords: nano iron oxide; *Phanerochaete chrysosporium*; oxidative stress; tetrabromobisphenol A

check for updates

Citation: Li, N.; Yu, J.; Wang, X.; Chen, L.; Jiang, H.; Zhang, W. Growth, Oxidative Stress and Ability to Degrade Tetrabromobisphenol A of *Phanerochaete chrysosporium* in the Presence of Different Nano Iron Oxides. *Water* **2024**, *16*, 567. https://doi.org/10.3390/w16040567

Academic Editors: Helvi Heinonen-Tanski and Reynaldo Patiño

Received: 23 January 2024
Revised: 10 February 2024
Accepted: 12 February 2024
Published: 14 February 2024

Copyright: © 2024 by the authors. Licensee MDPI, Basel, Switzerland. This article is an open access article distributed under the terms and conditions of the Creative Commons Attribution (CC BY) license (https://creativecommons.org/licenses/by/4.0/).

1. Introduction

Tetrabromobisphenol A (TBBPA) is one of the most widely used flame retardants in the production of plastics, textiles, and electronic circuit boards [1]. The widespread use of TBBPA has led to its detection in various environmental media such as air, dust, soil, water, sediment/sewage sludge, and even in food, organisms, and the human body [2]. With a deepened understanding of TBBPA, the World Health Organization's International Agency for Research on Cancer (IARC) classified it as a group 2A carcinogen in 2018. Therefore, effective and environmentally friendly TBBPA degradation technologies are urgently required. The biological treatment of TBBPA pollution is an attractive method for the degradation and conversion of TBBPA through microbial metabolism. White rot fungi are one kind of microorganism with strong organic matter degradation capability, and its degradation subjects range from lignocellulose to a variety of emerging organic pollutants, including the brominated flame retardant TBBPA [3]. However, not all strains of white rot fungi displayed good degradation effects on TBBPA; for example, *Phanerochaete chrysosporium* only degraded 20–40% of 1 mM TBBPA [1]. The performance of white rot fungi,

especially *Phanerochaete chrysosporium* in TBBPA degradation, needed to be enhanced and improved.

In recent years, more and more researchers have conducted investigations on the treatment of pollution with white rot fungi coupled with nanomaterials, where nano iron oxides were commonly used [4,5]. The remediation technique of white rot fungi synergized with nano iron oxides not only displayed better pollutant removal efficiency but also a higher degradation rate of organic pollutants. For example, Xu et al. prepared novel adsorbents with efficient Pb^{2+} adsorption by encapsulating Fe_3O_4 nanoparticles and calcium alginate in the mycelial spheres of *Phanerochaete chrysosporium* [6]. Moreover, Fe_3O_4 nanoparticles not only promoted lignocellulose degradation by *Phanerochaete chrysosporium* [7] but also promoted the degradation of phenol [8]. However, the degradation effect of TBBPA by *Phanerochaete chrysosporium* coupled with nano iron oxides is still unknown. Furthermore, the type of nano iron oxides used in previous studies was single, and more research is needed to assess the feasibility of other nano iron oxides when synergized with white rot fungi.

When nanomaterials coexisted with white rot fungi, this might have induced some physiological and metabolic changes in the microorganism, which further influenced the decomposition of organic compounds. For example, graphene oxide inhibited the biomass of white rot fungi [9]. CdSe/ZnS quantum dots induced meaningful increases in reactive oxygen species (ROS), malondialdehyde (MDA), superoxide (O_2^-), superoxide dismutase (SOD), and catalase (CAT) levels of *Phanerochaete chrysosporium*, suggesting oxidative damage [10]. As one common kind of metal oxide in nature, iron oxides have been considered safe for a long time, and the effects of nano iron oxides on microorganisms were negligible [11]. However, inherently non-toxic diamonds still aroused meaningful oxidative stress and induced the inhibition of decomposition activity in *Phanerochaete chrysosporium*. Furthermore, it has been found that the toxicity of nano iron oxides to wheat seedlings is related to their size and type [12]. Until now, the effects of different nano iron oxides on white rot fungi have been unclear, and it is necessary to perform specific studies on them.

In brief, in order to improve the performance of *Phanerochaete chrysosporium* in TBBPA degradation, the strategy of synergizing *Phanerochaete chrysosporium* with nano iron oxides was considered; however, the effects of different nano iron oxides on *Phanerochaete chrysosporium* are still unknown. Common iron oxide nanoparticles are α-Fe_2O_3, γ-Fe_2O_3, and Fe_3O_4 [13]. Therefore, this paper explored the effects of 20 nm γ-Fe_2O_3, 30 nm α-Fe_2O_3, 20 nm Fe_3O_4, and 200 nm Fe_3O_4 on *Phanerochaete chrysosporium* by monitoring the growth, oxidative stress, and the ability to degrade TBBPA of the fungus. This study could provide references for the further application of different iron oxides in the white rot fungal bioremediation of TBBPA.

2. Materials and Methods

2.1. Materials

In total, 20 nm of γ-Fe_2O_3, 30 nm of α-Fe_2O_3, 20 nm of Fe_3O_4, 200 nm of Fe_3O_4 and TBBPA (high purity 98%) were purchased from Shanghai Macklin Biochemical Co., Ltd., Shanghai, China. The hydrogen peroxide (H_2O_2) assay kit (spectrophotometric method), total superoxide dismutase (T-SOD) assay kit (hydroxylamine method), lactate dehydrogenase (LDH) assay kit (colorimetric method), microscale malondialdehyde (MDA) assay kit (colorimetric method) and catalase (CAT) assay kit (molybdenum amine method) were purchased from Nanjing Jiancheng Bioengineering Institute, Nanjing, China.

2.2. Strain and Culture Medium

The strain used in this experiment was *Phanerochaete chrysosporium* (BKMF-1767), which was provided by the China Centre for Type Culture Collection (CCTCC), with the collection number AF96007. The culture medium used can be referred to in our previous reports [14].

2.3. Inoculation Preparation

The spore suspension was prepared by scraping the spores with a sterilized cotton swab and dispersing them in sterilized water, which was mixed well. The spore concentration of the suspension was calculated by diluting and counting under a microscope. The concentration of the inoculation was adjusted to about 1×10^6 spore·mL^{-1}, and the absorbance of spore suspension at 650 nm was determined with a UV-visible spectrophotometer (UV-6100A, Shanghai Analytical Instrument Co., Ltd., Shanghai, China) in order to facilitate the repeated preparation of inoculation [15].

2.4. Culture Condition

The experiments were performed in 500 mL conical flasks with 200 mL of the culture medium. In the four experimental groups except the control group (CK group), 250 mg L^{-1} of 20 nm γ-Fe_2O_3, 30 nm α-Fe_2O_3, 20 nm Fe_3O_4, and 200 nm Fe_3O_4 were added to the culture medium, respectively. All the culture media were autoclaved at 121 °C for 30 min and cooled to room temperature, then inoculated with 2 mL of spore suspension, and then transferred to a thermostatic shaking incubator and incubated at 30 °C and 180 r·min^{-1} for 14 d. Three parallels were set for each group.

2.5. Measurement of Fungal Biomass

Samples were taken on days 3, 6, 8, 10, 12, and 14 and centrifuged at 4000 r·min^{-1} for 10 min to separate the supernatant from the fungal mycelium pellets. The dry weights of the fungal biomass were measured after being dried at 60 °C for 48 h.

2.6. Oxidative Stress Determination

Oxidative stress is the main recognized mechanism of the biotoxicity of nanomaterials, which could affect the normal activities of cells and even lead to the death of cells in severe cases [16]. In order to reveal the possible toxicological mechanisms of nano iron oxides against *Phanerochaete chrysosporium*, the content of intracellular reactive oxygen species H_2O_2, the activity of antioxidant enzymes CAT and SOD, the activity of LDH, and the content of MDA, both of which could characterize the degree of cell membrane damage, were measured.

After 14 d of culture, the mycelium pellets and the culture supernatant were separated from the culture medium via centrifugation. The culture supernatant was used for the assay of LDH enzyme activity according to the instructions of the LDH kit. Pyruvic acid catalyzed from lactic acid via LDH reacted with 2,4-dinitrophenylhydrazine to produce pyruvate dinitrophenylhydrazone, which was brownish-red in alkaline solutions, and the color depth was proportional to the pyruvate concentration. The activity of LDH could be calculated by measuring the optical density (OD) value of the brownish-red solution at 440 nm.

The mycelium pellets were washed twice with phosphate-buffered saline (PBS), which was sterilized and precooled to 4 °C [17], and then filter paper was used to remove the apparent water of fungal mycelium pellets. In total, 0.25 g of the fungal mycelium pellets were accurately weighed and placed in a 2 mL centrifuge tube, and then 1 mL of PBS and the grinding beads were added to the tubes. The mixture was ground for 5 min with an automatic rapid grinding machine (JXFSTPRP-48, Shanghai Jingxin Industrial Development Co. Ltd., Shanghai, China), and it was chilled with iced water for 1 min every 1 min of grinding. After grinding, the samples were centrifuged at 10,000 r·min^{-1}, at 4 °C for 10 min (if the supernatant was still turbid, it could be centrifuged again), and the corresponding supernatant was collected to determine the intracellular H_2O_2 content, CAT activity, SOD activity and MDA content, which were all determined in strict accordance with the steps of the kit instructions. The H_2O_2 content was calculated based on the interaction of H_2O_2 with molybdic acid to form a complex that could be detected at 405 nm. The activity of CAT was determined by the addition of ammonium molybdate, and the decomposition of H_2O_2 rapidly stopped while ammonium molybdate reacted with the remaining H_2O_2 to

form a yellowish complex and was calculated by its absorbance at 405 nm. SOD activity was measured by the repression of the enzyme extract on superoxide anon free radicals, which reduced the formation of nitrite, resulting in the absorbance value at a wavelength of 550 nm lower than that of the control. The MDA content was measured based on the condensation reaction of MDA, and thiobarbituric acid formed a red product with a maximum absorption peak at 532 nm.

2.7. Degradation and Adsorption of TBBPA by Phanerochaete chrysosporium Coupled with Different Nano Iron Oxides

This experiment was performed in 200 mL conical flasks with 100 mL of the culture medium. Except for the control group (CK group), four experimental groups with the addition of 250 mg·L^{-1} of 20 nm γ-Fe_2O_3, 30 nm α-Fe_2O_3, 20 nm Fe_3O_4, and 200 nm Fe_3O_4, respectively, were set. During the 6 d culture, 20 mg·L^{-1} of TBBPA was added on day 3. Three parallels were set for each group, and samples were taken on day 6. In the process of culture, almost all the nano iron oxides were adsorbed on the fungal mycelia. The fungal mycelium and culture supernatant were separated by centrifugation at 4000 r·min^{-1} for 10 min. The mycelia were added to 10 mL of a 0.1 mol·L^{-1} sodium hydroxide (NaOH)solution and mixed at 30 °C, 180 r·min^{-1} for 1 h, and then centrifuged at 4000 r·min^{-1} for 10 min to obtain the supernatant, and then filtered through a 0.22 μm organic filtration membrane. The culture supernatant was shaken well, and the pH was adjusted to 9 with 1 mol·L^{-1} of the NaOH solution to dissolve TBBPA completely, which was then filtered through a 0.22 μm organic filtration membrane. The TBBPA content in the filtrates originated from mycelium and was defined as the adsorbed TBBPA moiety, and the TBBPA content in the filtrates originating from culture supernatant was defined as the TBBPA moiety left in the culture medium.

The filtrates originated from the mycelium and culture supernatant were both used for TBBPA determination with the high performance of the liquid chromatograph (HPLC, Agilent 1260), and the detection conditions were as follows: ZORBAX Rx-C18 column (4.6 × 250 mm, 5 um, 400 bar pressure limit), an injection volume of 20 μL, flow rate at 1 mL·min^{-1}, column temperature at 35 °C, the mobile phase consisted of methanol and glacial acetic acid solution (0.5% acetic acid) at 85:15 (*v*:*v*), and a detection wavelength of 290 nm.

2.8. Statistical Analysis

All the experiments were conducted with at least 3 parallels, and the results were expressed as the mean ± standard deviation. The differences between the treatments were analyzed by one-way analysis of variance (ANOVA) with a multiple comparison test (Dunnet's, Least Significant Difference (LSD) and Student–Newman–Keuls (S–N–K)) at the 5% significant level. The statistical analysis was performed by SPSS 27.0.

3. Results and Discussion

3.1. Changes in Biomass of Phanerochaete chrysosporium

The measurements of dry weight could reflect the effect of nano iron oxides on the growth of *Phanerochaete chrysosporium*. As shown in Figure 1, the dry weights of *Phanerochaete chrysosporium* increased rapidly from 0 d to 6 d, especially from 0 d to 3 d. This stage was the rapid growth period of *Phanerochaete chrysosporium*, and the biomass started to fluctuate up and down after 6 d. At 14 d, it was observed that the dry weights in most experimental groups were higher than that in the CK group, but these increases were not significant compared to those in the CK group. There were no significant differences between different groups at the same incubation time, and the hardly decreased biomass in the coculture of *Phanerochaete chrysosporium* with different nano iron oxides both demonstrated that the four nano iron oxides had little or almost no inhibition on the growth of *Phanerochaete chrysosporium*. This was similar to the effect of graphene [18], carbon nan-

otubes [19], pristine fullerene [18], or the nano diamond [20] on the fresh and dry weights of white rot fungi.

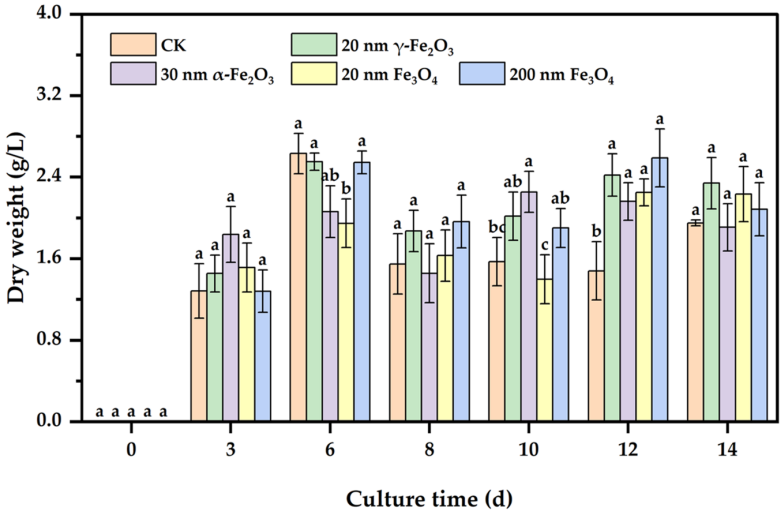

Figure 1. Effect of nano iron oxides on the growth of *Phanerochaete chrysosporium*. Different letters indicated significant differences between the treatments ($p < 0.05$).

3.2. Effect of Nano Iron Oxides on Oxidative Stress in Phanerochaete chrysosporium

3.2.1. Intracellular H_2O_2 Content

H_2O_2 is one common reactive oxygen species produced in the process of cell growth and metabolism. Studies have shown that excess reactive oxygen species attacked key cellular components, causing a series of toxic effects such as lipid peroxidation, mitochondrial dysfunction, and DNA damage [21]. When cells are subjected to environmental stress, the intracellular H_2O_2 content increases sharply and forms clear oxidative pressure on cells, resulting in oxidative damage [22]. Therefore, the detection of intracellular reactive oxygen species content is important for assessing cellular oxidative stress. As shown in Figure 2, the 20 nm γ-Fe_2O_3 and 30 nm α-Fe_2O_3 groups significantly increased the intracellular H_2O_2 content compared with the control group, whereas the addition of Fe_3O_4 with different sizes had no significant effect on the intracellular H_2O_2 content. The results show that more H_2O_2 was induced by nano Fe_2O_3 than by nano Fe_3O_4, and smaller iron oxides. A higher intracellular H_2O_2 content indicated higher oxidative pressure [23], and not all nano iron oxides induced higher oxidative pressure in *Phanerochaete chrysosporium*, such as 200 nm Fe_3O_4.

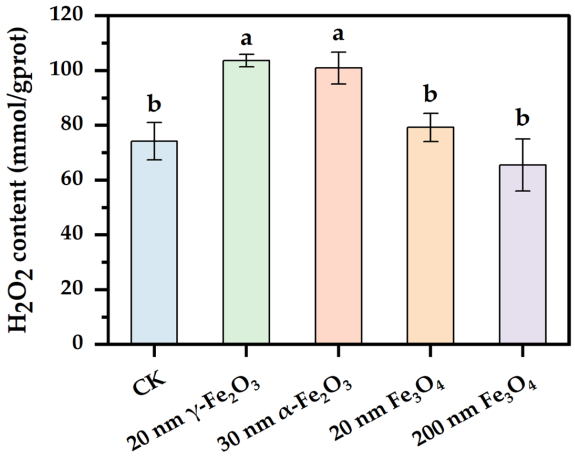

Figure 2. Effect of nano iron oxides on the content of H_2O_2 in the cell of *Phanerochaete chrysosporium*. Different letters indicated significant differences between the treatments ($p < 0.05$).

3.2.2. Intracellular SOD and CAT Activities

An antioxidant defense system was developed in organisms to scavenge excess viable oxygen species timely before damage was caused to intracellular components, thus mitigating the toxic effects of oxidative stress on organisms [24]. Antioxidant enzymes are the main composition in the antioxidant defense system, and SOD and CAT are two functional enzymes involved in antioxidant defense [25]. The effects of different nano iron oxides on the intracellular activities of SOD and CAT in *Phanerochaete chrysosporium* are shown in Figure 3. As shown in Figure 3A, the 20 nm Fe_3O_4 group, 30 nm α-Fe_2O_3 group and 20 nm γ-Fe_2O_3 group significantly inhibited intracellular SOD activity compared to the control group, with the most significant one being the 20 nm γ-Fe_2O_3 group, whereas there was no significant difference between the 200 nm Fe_3O_4 group and the control group, where even the intracellular SOD activity was a little higher in the 200 nm Fe_3O_4 group than the control group. In Figure 3B, there were significant differences between both the control and nano iron oxides groups, in which the 200 nm Fe_3O_4 group significantly increased the intracellular CAT activity, while the 20 nm Fe_3O_4 group, the 30 nm α-Fe_2O_3 group and the 20 nm γ-Fe_2O_3 group significantly inhibited the intracellular CAT activity. The two antioxidant enzymes had a synergistic effect in resisting oxidative stress, with SOD first converting superoxide anion radicals to H_2O_2, before CAT completely detoxified H_2O_2 to H_2O and O_2 [23]. The results demonstrated that the addition of nano iron oxides except 200 nm Fe_3O_4 probably induced the consumption or the inhibition of SOD and CAT in *Phanerochaete chrysosporium*, and these changes were more significant in the group with a smaller size Fe_2O_3.

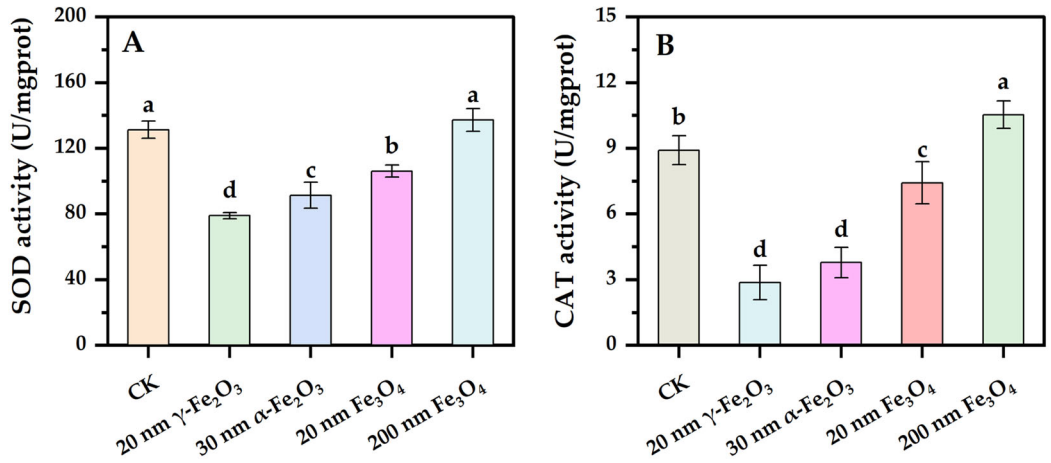

Figure 3. Effect of nano iron oxides on SOD and CAT activities of *Phanerochaete chrysosporium* ((**A**): SOD, (**B**): CAT). Different letters indicated significance of differences between the treatments ($p < 0.05$).

3.2.3. Extracellular LDH Activity and Intracellular MDA Content

Changes in the permeability of the cell membrane are early responses to the toxicity of nanoparticles [26]. LDH is a cytosolic enzyme that can be outside the cell when the cell membrane is damaged or its permeability is increased, resulting in a significant increase in extracellular LDH activity. Extracellular LDH activity is capable of sensitively reflecting the damage degree of the cell membrane as well as changes in the permeability of the cell membrane. The results of the extracellular LDH assay are shown in Figure 4A. Except for the 200 nm Fe_3O_4 group, there were significant differences between all the nano iron oxide groups and the control group. Extracellular LDH activity was significantly increased in the 20 nm γ-Fe_2O_3 group, 30 nm α-Fe_2O_3 group and 20 nm Fe_3O_4 group compared with the control group. Similar to the changes in intracellular H_2O_2 content, higher extracellular LDH activity was induced by nano Fe_2O_3, and smaller size iron oxide, while Fe_2O_3 with different crystal types did not lead to significant differences in extracellular LDH activity.

The results probably illustrated an increase in the permeability of the cell membrane of *Phanerochaete chrysosporium* induced by the addition of four nano iron oxides, and different degrees of damage were brought by different particle sizes and types of nano iron oxide, which corresponded with the size effect of nanomaterials and the smaller the size of the nanomaterials, the higher the surface viability and toxicity, and the greater the damage of the materials to the microorganisms [27].

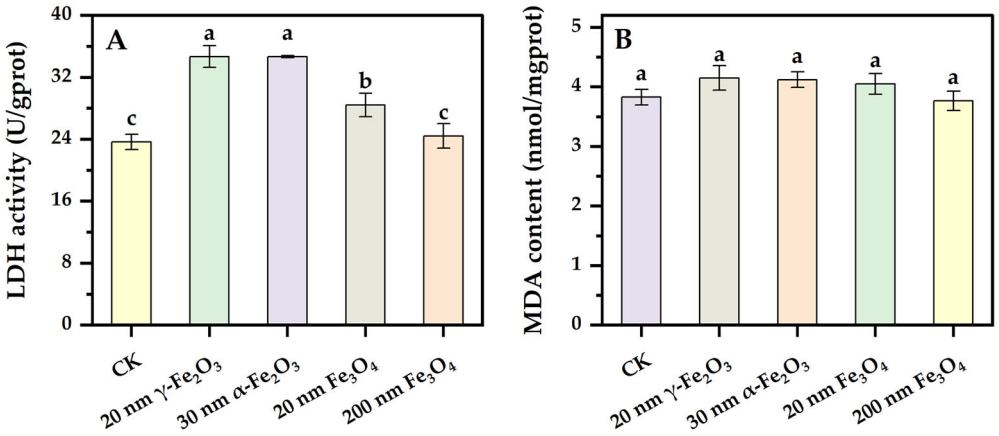

Figure 4. Effect of nano iron oxides on extracellular LDH activity and intracellular MDA content in *Phanerochaete chrysosporium* ((**A**): LDH, (**B**): MDA). Different letters indicated significant differences between the treatments ($p < 0.05$).

MDA is the final product of lipid peroxidation, and the intracellular MDA level is often used to measure the degree of lipid peroxidation [21]. Typically, the excessive intracellular accumulation of viable oxygen species interacts with enzymes on biological membranes, membrane receptors, and the polyunsaturated fatty acid side chains of phospholipids to cause lipid peroxidation. The effects of different nano iron oxides on the intracellular MDA content of *Phanerochaete chrysosporium* are shown in Figure 4B. There was no significant difference in MDA concentration between the groups, but the intracellular MDA content was a little higher in the nano iron oxide groups than in the CK group. The degree of lipid peroxidation in the membrane was closely related to the content of reactive oxygen species, and antioxidant enzymes could help to reduce the damage of reactive oxygen species on cells. Compared with the changes in LDH activity, it probably illustrates that the changes in the permeability of the cell membrane were more significantly affected by the addition of iron oxides than the degree changes in lipid peroxidation.

Combining all the above data on oxidative stress, it was found that the toxic effect induced by 200 nm Fe_3O_4 was weakest, only resulting in slightly higher intracellular CAT activity, which was probably due to the effective antioxidant defense system of *Phanerochaete chrysosporium*, which could cope with almost all oxidative pressure induced by this nanoparticle. But when the size of nano iron oxide became significantly smaller, lower intracellular SOD and CAT activities and higher extracellular LDH activity were induced. When the type of iron oxide changed from Fe_3O_4 to Fe_2O_3, the oxidative stress induced by the iron oxides was too great for the antioxidant system to resist, and the antioxidant property became weakened, so this resulted in a much higher level of intracellular H_2O_2 content and oxidative stress. The relationships between oxidative stress parameters are shown in Table S1. Statistically significant correlations were found between the oxidative stress parameters. H_2O_2 was negatively correlated with SOD and CAT and positively correlated with LDH and MDA.

3.3. Degradation and Adsorption of TBBPA by Phanerochaete chrysosporium Coupled with Different Nano Iron Oxides

The removal process of organic matter by white-rot fungi usually involves both adsorption and degradation processes, and nano iron oxides are good adsorbents of TBBPA [28]; therefore, it is necessary to differentiate between the removal efficiency and the degradation efficiency of TBBPA by *Phanerochaete chrysosporium* coupled with different nano iron oxides. As shown in Figure 5, it was observed that the removal process of TBBPA was mainly due to degradation with little adsorption. After 3 d of degradation, all the nano iron oxide groups significantly contributed to the removal of TBBPA compared to the control group (Figure 5A). The degradation rate of TBBPA in all five groups was more than 87% and contributed to about 96% of TBBPA removal. The degradation rate of TBBPA by *Phanerochaete chrysosporium* was significantly higher than that reported above by Uhnáková et al., which might be due to the different species of *Phanerochaete chrysosporium* [1]. Nano iron oxides had a good adsorption effect on TBBPA [28], and these adsorption effects were related to the particle size, but the above experimental results show that nano iron oxide synergized with *Phanerochaete chrysosporium* did not show a significant adsorption effect on TBBPA, which probably was due to the fact that the production of extracellular polymeric substances by *Phanerochaete chrysosporium* changed the surface properties of nano iron oxides [29]. Nevertheless, the adsorption of TBBPA coupled with nano iron oxides was significantly higher than that by *Phanerochaete chrysosporium* in pure culture (Figure 5B). The fungal mycelium showed some adsorption effect on TBBPA but did not show a higher adsorption efficiency with increasing biomass. The above results indicate that the strategy where *Phanerochaete chrysosporium* couples with different nano iron oxides could remove and degrade TBBPA well.

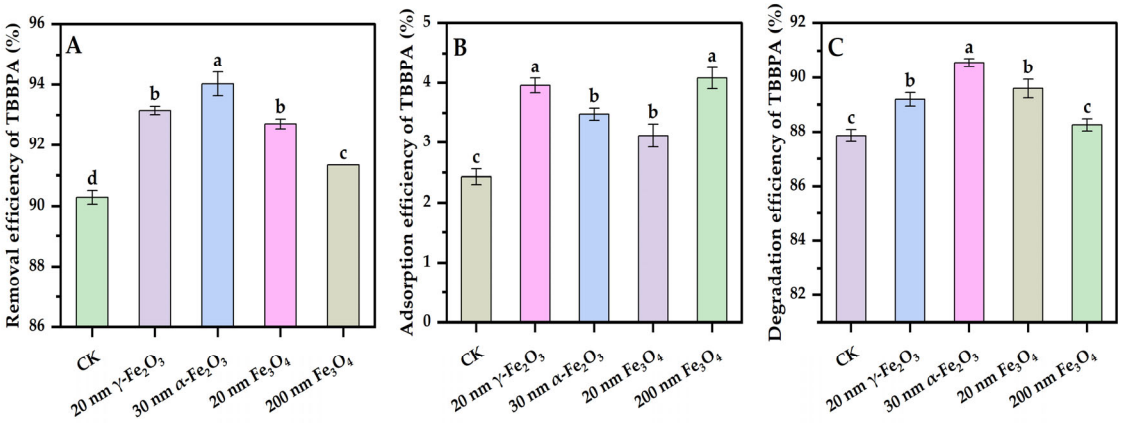

Figure 5. Effects of nano iron oxides on the removal (**A**), adsorption (**B**), and degradation (**C**) of TBBPA using *Phanerochaete chrysosporium.* Different letters indicated significant differences between the treatments ($p < 0.05$).

As seen from Figure 5C, after 3 d of degradation, the 20 nm γ-Fe_2O_3 group, the 30 nm α-Fe_2O_3 group, and the 20 nm Fe_3O_4 group all significantly promoted the degradation of TBBPA compared with the control group. However, due to the excellent performance of TBBPA degradation by pure-cultured *Phanerochaete chrysosporium*, the highest enhancement of TBBPA's degradation efficiency using different nano iron oxides was only 2.7%. This suggests that the addition of nano iron oxides only had a weak enhancement effect on the degradation of TBBPA, and this enhancement effect was related to the type of iron oxides, with the smaller particle sizes of iron oxides and α-Fe_2O_3 having a relatively more pronounced enhancement effect. In the degradation process of TBBPA, only the activities of LiP and MnP were detected without clear Lac activity (Figure S1). Although the degradation of organic matter by white rot fungi largely depends on enzyme activity [30], there was no significant correlation between the changes in lignin-degrading enzyme activities

and TBBPA degradation efficiency (Table S2), with higher activities of LiP and MnP in the 200 nm Fe_3O_4 group and no clear enhancement of the degradation efficiency of TBBPA. The above results demonstrate that there were other mechanisms affecting the degradation of TBBPA. The higher lignin-degradation enzyme activities did not result in the higher degradation efficiency of norfloxacin, as was also found before, which was due to the inhibition of the intracellular cytochrome P450 [14]. The involvement of intracellular cytochrome P450 in TBBPA degradation was demonstrated in the degradation experiment of TBBPA using *Phanerochaete chrysosporium* with the addition of cytochrome P450 enzyme inhibitors piperonyl butoxide (PB). The degradation efficiency of TBBPA using *Phanerochaete chrysosporium* decreased clearly when PB was present (Figure S2). Li et al. [31] also found that the addition of γ-Fe_2O_3 alone did not have a promoting effect on the degradation of bisphenol A using white rot fungi, and only with the exogenous addition of hydrogen peroxide at the same time could the degradation efficiency be significantly improved. A higher intracellular H_2O_2 content was detected in groups with smaller iron oxides (Figure 2); the correlation coefficient between TBBPA degradation and the intracellular H_2O_2 concentration was 0.815, but the correlation was not significant (Table S2).

4. Conclusions

The effects of 20 nm γ-Fe_2O_3, 30 nm α-Fe_2O_3, 20 nm Fe_3O_4, and 200 nm Fe_3O_4 on *Phanerochaete chrysosporium* were explored by monitoring the growth, oxidative stress, and ability to degrade the TBBPA content of the fungus. The four nano iron oxides did not inhibit the growth of *Phanerochaete chrysosporium*. However, the oxidative stress of *Phanerochaete chrysosporium* induced by nano iron oxides was not only size-dependent but also type-dependent. *Phanerochaete chrysosporium* and nano iron oxides could synergistically improve the removal rate of TBBPA, with smaller iron oxides showing a relatively higher enhancement in the degradation of TBBPA, and this enhanced degradation effect has no significant correlation with lignin-degrading enzyme activities but was closely correlated with the intracellular H_2O_2 concentration.

Supplementary Materials: The following supporting information can be downloaded at: https://www.mdpi.com/article/10.3390/w16040567/s1. Figure S1: The activities of lignin-degrading enzymes produced using Phanerochaete chrysosporium after 3 days of TBBPA degradation (A: LiP, B: MnP); Figure S2: Effect of cytochrome P450 inhibitor PB on TBBPA degradation using Phanerochaete chrysosporium; Table S1: Correlation coefficients of oxidative stress parameters of Phanerochaete chrysosporium; Table S2: Correlation coefficients for removal, adsorption and degradation of TBBPA and extracellular lignin-degrading enzymes activities using Phanerochaete chrysosporium. Reference [30] is cited in the Supplementary Materials.

Author Contributions: Conceptualization, N.L., J.Y. and X.W.; methodology, J.Y.; software, L.C.; validation, J.Y. and X.W.; formal analysis, X.W.; investigation, J.Y. and X.W.; resources, N.L.; data curation, L.C.; writing—original draft preparation, J.Y.; writing—review and editing, J.Y., X.W., L.C. and H.J.; visualization, J.Y.; supervision, N.L.; project administration, W.Z.; funding acquisition, N.L. All authors have read and agreed to the published version of the manuscript.

Funding: This research was supported by the National Natural Science Foundation of China (Grant number: 51608142), the Natural Science Foundation Project of Guangxi Province (Grant number: 2018GXNSFGA281001, 2016GXNSFBA380076), and the Science and Technology Base and Talent Project of Guangxi (Grant number: AD19110151).

Data Availability Statement: The data presented in this study are available on request from the corresponding author.

Acknowledgments: We thank Xuezhen Zhang, Shiqi Chen, Qingkun Han, and Luyang Wang for their help with the analysis.

Conflicts of Interest: The authors declare no conflicts of interest.

References

1. Uhnáková, B.; Ludwig, R.; Pěknicová, J.; Homolka, L.; Lisá, L.; Šulc, M.; Petříčková, A.; Elzeinová, F.; Pelantová, H.; Monti, D.; et al. Biodegradation of tetrabromobisphenol A by oxidases in basidiomycetous fungi and estrogenic activity of the biotransformation products. *Bioresour. Technol.* **2011**, *102*, 9409–9415. [CrossRef] [PubMed]
2. Jiang, Y.; Wang, L.; Zheng, M.; Lin, Y.; Liu, A.; Wang, Y.; Li, Y. Identification of lower brominated bisphenol A analogs as the photooxidation products of tetrabromobisphenol A bis(2,3-dibromopropyl) ether (TBBPA-BDBPE). *Sci. Total Environ.* **2023**, *890*, 164227. [CrossRef] [PubMed]
3. Chen, J.; Wu, J.; Fan, L.; Jia, R. Studies on the characteristics and mechanism of aerobic biodegradation of tetrabromobisphenol A by *Irpex lacteus* F17. *J. Basic Microbiol.* **2021**, *61*, 419–429. [CrossRef] [PubMed]
4. Khoso, W.A.; Haleem, N.; Baig, M.A.; Jamal, Y. Synthesis, characterization and heavy metal removal efficiency of nickel ferrite nanoparticles (NFN's). *Sci. Rep.* **2021**, *11*, 3790. [CrossRef] [PubMed]
5. Geetha, K.; Udhayakumar, R.; Manikandan, A. Enhanced magnetic and photocatalytic characteristics of cerium substituted spinel $MgFe_2O_4$ ferrite nanoparticles. *Phys. B Condens. Matter* **2021**, *615*, 413083. [CrossRef]
6. Xu, P.; Zeng, G.M.; Huang, D.L.; Lai, C.; Zhao, M.H.; Wei, Z.; Li, N.J.; Huang, C.; Xie, G.X. Adsorption of Pb (II) by iron oxide nanoparticles immobilized *Phanerochaete chrysosporium*: Equilibrium, kinetic, thermodynamic and mechanisms analysis. *Chem. Eng. J.* **2012**, *203*, 423–431. [CrossRef]
7. Huang, D.; Li, T.; Xu, P.; Zeng, G.; Chen, M.; Lai, C.; Cheng, M.; Guo, X.; Chen, S.; Li, Z. Deciphering the Fenton-reaction-aid lignocellulose degradation pattern by *Phanerochaete chrysosporium* with ferroferric oxide nanomaterials: Enzyme secretion, straw humification and structural alteration. *Bioresour. Technol.* **2019**, *276*, 335–342. [CrossRef]
8. Huang, D.-L.; Wang, C.; Xu, P.; Zeng, G.-M.; Lu, B.-A.; Li, N.-J.; Huang, C.; Lai, C.; Zhao, M.-H.; Xu, J.-J.; et al. A coupled photocatalytic-biological process for phenol degradation in the *Phanerochaete chrysosporium*-oxalate-Fe_3O_4 system. *Int. Biodeterior. Biodegrad.* **2015**, *97*, 115–123. [CrossRef]
9. Xie, J.; Ming, Z.; Li, H.; Yang, H.; Yu, B.; Wu, R.; Liu, X.; Bai, Y.; Yang, S.-T. Toxicity of graphene oxide to white rot fungus *Phanerochaete chrysosporium*. *Chemosphere* **2016**, *151*, 324–331. [CrossRef]
10. Hu, L.; Wan, J.; Zeng, G.; Chen, A.; Chen, G.; Huang, Z.; He, K.; Cheng, M.; Zhou, C.; Xiong, W.; et al. Comprehensive evaluation of the cytotoxicity of CdSe/ZnS quantum dots in *Phanerochaete chrysosporium* by cellular uptake and oxidative stress. *Environ. Sci. Nano* **2017**, *4*, 2018–2029. [CrossRef]
11. Zhang, L.; Dong, H.; Zhang, J.; Chen, Y.; Zeng, G.; Yuan, Y.; Cao, W.; Fang, W.; Hou, K.; Wang, B.; et al. Influence of FeONPs amendment on nitrogen conservation and microbial community succession during composting of agricultural waste: Relative contributions of ammonia-oxidizing bacteria and archaea to nitrogen conservation. *Bioresour. Technol.* **2019**, *287*, 121463. [CrossRef]
12. Cheng, Y.; Cheng, Y.; Zheng, H.; Song, Y.; Li, R.; Wan, F.; Li, J. Evaluation and Comparison of the Toxic Effects of MgO NPs, ZnO NPs, α-Fe_2O_3 NPs, γ-Fe_2O_3 NPs, and Fe_3O_4 NPs on the Remediation for Cadmium-Related Effects in Wheat Seedlings. *Water Air Soil Pollut.* **2020**, *231*, 471. [CrossRef]
13. Voss, L.; Yilmaz, K.; Burkard, L.; Vidmar, J.; Stock, V.; Hoffmann, U.; Pötz, O.; Hammer, H.S.; Peiser, M.; Braeuning, A.; et al. Impact of iron oxide nanoparticles on xenobiotic metabolism in HepaRG cells. *Arch. Toxicol.* **2020**, *94*, 4023–4035. [CrossRef] [PubMed]
14. Chen, Z.; Li, N.; Lan, Q.; Zhang, X.; Wu, L.; Liu, J.; Yang, R. Laccase inducer Mn^{2+} inhibited the intracellular degradation of norfloxacin by *Phanerochaete chrysosporium*. *Int. Biodeterior. Biodegrad.* **2021**, *164*, 105300. [CrossRef]
15. Pellinen, J.; Abuhasan, J.; Joyce, T.W.; Chang, H.M. Biological delignification of pulp by *Phanerochaete chrysosporium*. *J. Biotechnol.* **1989**, *10*, 161–170. [CrossRef]
16. Wang, Y.; Cai, R.; Chen, C. The Nano–Bio Interactions of Nanomedicines: Understanding the Biochemical Driving Forces and Redox Reactions. *Acc. Chem. Res.* **2019**, *52*, 1507–1518. [CrossRef] [PubMed]
17. Mi, F.; Jiahua, Z.; Jun, Z.; Yuanyu, Y.; Yushou, G. The performance and mechanism of triphenyl phosphate biodegradation by *Phanerochaete chrysosporium*. *China Environ. Sci.* **2020**, *40*, 4919–4926.
18. Ming, Z.; Feng, S.; Yilihamu, A.; Ma, Q.; Yang, S.; Yang, S.-T. Toxicity of Pristine and Chemically Functionalized Fullerenes to White Rot Fungus *Phanerochaete chrysosporium*. *Nanomaterials* **2018**, *8*, 120. [CrossRef] [PubMed]
19. Ming, Z.; Feng, S.; Yilihamu, A.; Yang, S.; Ma, Q.; Yang, H.; Bai, Y.; Yang, S.T. Toxicity of carbon nanotubes to white rot fungus *Phanerochaete chrysosporium*. *Ecotoxicol. Environ. Saf.* **2018**, *162*, 225–234. [CrossRef]
20. Ma, Q.; Zhang, Q.; Yang, S.; Yilihamu, A.; Shi, M.; Ouyang, B.; Guan, X.; Yang, S.T. Toxicity of nanodiamonds to white rot fungi *Phanerochaete chrysosporium* through oxidative stress. *Colloids Surf. B Biointerfaces* **2020**, *187*, 110658. [CrossRef]
21. Lee, J.; Hwang, J.-S.; Hwang, I.-S.; Cho, J.; Lee, E.; Kim, Y.; Lee, D.G. Coprisin-induced antifungal effects in *Candida albicans* correlate with apoptotic mechanisms. *Free. Radic. Biol. Med.* **2012**, *52*, 2302–2311. [CrossRef]
22. Chen, Z.; Song, S.; Wen, Y.; Zou, Y.; Liu, H. Toxicity of Cu (II) to the green alga *Chlorella vulgaris*: A perspective of photosynthesis and oxidant stress. *Environ. Sci. Pollut. Res. Int.* **2016**, *23*, 17910–17918. [CrossRef] [PubMed]
23. Feng, M.; Yin, H.; Peng, H.; Liu, Z.; Lu, G.; Dang, Z. Hexavalent chromium induced oxidative stress and apoptosis in *Pycnoporus sanguineus*. *Environ. Pollut.* **2017**, *228*, 128–139. [CrossRef] [PubMed]
24. Wu, Y.; Wang, Y.; Du, J.; Wang, Z.; Wu, Q. Effects of yttrium under lead stress on growth and physiological characteristics of *Microcystis aeruginosa*. *J. Rare Earths* **2016**, *34*, 747–756. [CrossRef]

25. Jiang, J.; Liu, H.; Li, Q.; Gao, N.; Yao, Y.; Xu, H. Combined remediation of Cd–phenanthrene co-contaminated soil by *Pleurotus cornucopiae* and *Bacillus thuringiensis* FQ1 and the antioxidant responses in *Pleurotus cornucopiae*. *Ecotoxicol. Environ. Saf.* **2015**, *120*, 386–393. [CrossRef] [PubMed]
26. Shuihua, Z.; Qibing, M.; Jing, M. Toxicity study of iron tetroxide nanoparticles and carbon nanotubes on A549 cells. *J. Toxicol.* **2008**, *22*, 365–367.
27. Wei, B.; Chengcheng, Z.; Wenjun, J.; Zhiyong, Z.; Yuliang, Z. Progress in studies on environmental behaviors and toxicological effects of nanomaterials. *Asian J. Ecotoxicol.* **2009**, *4*, 174–182.
28. Zhou, Q.; Wang, Y.; Xiao, J.; Zhan, Y. Preparation of magnetic core-shell Fe_3O_4@polyaniline composite material and its application in adsorption and removal of tetrabromobisphenol A and decabromodiphenyl ether. *Ecotoxicol. Environ. Saf.* **2019**, *183*, 109471. [CrossRef]
29. Li, N.; Liu, J.; Yang, R.; Wu, L. Distribution, characteristics of extracellular polymeric substances of *Phanerochaete chrysosporium* under lead ion stress and the influence on Pb removal. *Sci. Rep.* **2020**, *10*, 17633. [CrossRef]
30. Wang, S.; Li, W.; Liu, L.; Qi, H.; You, H. Biodegradation of decabromodiphenyl ethane (DBDPE) by white-rot fungus *Pleurotus ostreatus*: Characteristics, mechanisms, and toxicological response. *J. Hazard. Mater.* **2022**, *424*, 127716. [CrossRef]
31. Li, M.; Zhang, C. γ-Fe_2O_3 nanoparticle-facilitated bisphenol A degradation by white rot fungus. *Sci. Bull.* **2016**, *61*, 468–472. [CrossRef]

Disclaimer/Publisher's Note: The statements, opinions and data contained in all publications are solely those of the individual author(s) and contributor(s) and not of MDPI and/or the editor(s). MDPI and/or the editor(s) disclaim responsibility for any injury to people or property resulting from any ideas, methods, instructions or products referred to in the content.